

D. Ljung, C. Pascaud, S. Pruss, W. M. Smart, H. H. Bingham, D. M. Chew, B. Y. Daugeras, W. B. Fretter, G. Goldhaber, W. R. Graves, A. D. Johnson, J. A. Kadyk, L. Stutte, G. H. Trilling, F. C. Winkelmann, and G. P. Yost, paper submitted to the Seventeenth International Conference on High Energy Physics, London, England, 1974 (unpublished).

<sup>8</sup>For review articles on  $pp$  and  $\pi^-p$  production of neutral particles at high energy see D. Ljung, in *Particles*

and *Fields—1973*, AIP Conference Proceedings No. 14, edited by H. H. Bingham, M. Davier, and G. R. Lynch (American Institute of Physics, New York, 1974), p. 464; J. Whitmore, *Phys. Rep.* **10**, 273 (1974).

<sup>9</sup>W. T. Ko, in *Proceedings of the Seventeenth International Conference on High Energy Physics, London, England, 1-76 1974*, edited by J. R. Smith (Rutherford High Energy Laboratory, Didcot, Berkshire, England, 1975).

### Pion-<sup>4</sup>He Scattering around the $\frac{3}{2}, \frac{3}{2}$ Resonance

F. Binon, P. Duteil, M. Gouanère, L. Hugon,\* J. Jansen, J.-P. Lagnaux, H. Palevsky,†  
J.-P. Peigneux, M. Spighel, and J.-P. Stroot  
[IISN (Belgium)-IPN (Orsay) Collaboration]

*Institut Interuniversitaire des Sciences Nucléaires, Belgium, and CERN, Geneva, Switzerland, and  
Institut de Physique Nucléaire, Faculté des Sciences, Orsay, France, and  
Faculté des Sciences, Clermont-Ferrand, France*

(Received 3 March 1975)

We present  $\pi^-$ -<sup>4</sup>He differential cross sections at 110, 150, 180, 220, and 260 MeV, as well as total cross sections at eleven energies between 67 and 285 MeV.

Negative-pion-<sup>4</sup>He scattering has been measured at the CERN synchrocyclotron with the double achromatic spectrometer previously used for pion-<sup>12</sup>C scattering.<sup>1,2</sup> A liquid-helium target of the supercooled type with a precise temperature regulation was installed for these measurements. Its windows consisted of thin Havar (Co-Fe) foils, except for the very-forward-angle measurements, where Mylar windows were used because of their lower atomic number. Effective target thicknesses are extrapolated from window-bulge measurements made at room temperature under controlled pressure conditions. The relative error of this procedure is  $\pm 3\%$ . It is the main contribution to the total relative error on the absolute normalization of the data which is estimated to be  $\pm 4\%$ .

Momentum dispersion of the incident pion beam was  $\Delta p/p = \pm 1.8\%$ . Overall angular resolution was  $1^\circ$  with use of a setup which included a DISC counter for identifying the forward-scattered pions. It was  $2^\circ$  for the large-angle measurements.

The experimental data are represented in Fig. 1. Differential cross sections are given as a function of the scattering angle in the center-of-mass system.

Cross sections for  $180^\circ$  scattering were measured by observing <sup>4</sup>He nuclei recoiling in the forward direction. For this purpose, the target

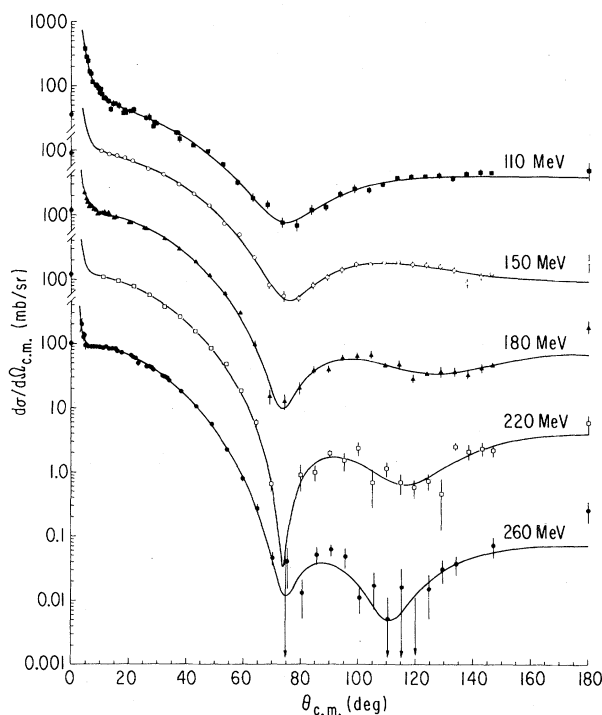


FIG. 1.  $\pi^-$ -<sup>4</sup>He elastic-scattering differential cross sections versus  $\theta_{c.m.}$ , the pion scattering angle in the c.m. system. Optical points on vertical axis show the value of  $(k/4\pi)|\text{Im}f|^2$  as deduced from our measured total cross sections. Only part of the forward data are shown for the sake of clarity. The curves result from fits by a formula given in the text.

was filled with helium gas under pressure and temperature conditions such that recoil  $\alpha$  particles had still enough energy to traverse the detectors placed at the entrance of the analyzing spectrometer and at its focal plane. These detectors were low-pressure multiwire proportional chambers<sup>3</sup> filled with pentane at a pressure of 6 Torr. The trajectories of the particles were in this case completely in vacuum. Unexpected difficulties arose in determining the absolute efficiency of these detectors.<sup>4</sup> The differential cross sections for pion scattering at  $180^\circ$  were finally deduced from the following scaling:

$$\left(\frac{d\sigma(180^\circ)}{d\Omega}\right)_{\text{c.m.}}^\pi = \left(\frac{d\sigma(146.8^\circ)}{d\Omega}\right)_{\text{c.m.}}^\pi \frac{[d\sigma(0^\circ)/d\Omega]_{\text{c.m.}}^\alpha}{[d\sigma(33.2^\circ)/d\Omega]_{\text{c.m.}}^\alpha},$$

where  $146.8^\circ$  is the angle in the c.m. system corresponding to the maximum angle in the laboratory at which the spectrometer could be rotated, namely  $144^\circ$ , and  $33.2^\circ$  is the corresponding angle in the c.m. for the recoiling  $\alpha$ 's.

Total cross sections are represented in Fig. 2, together with experimental results from Wilkin

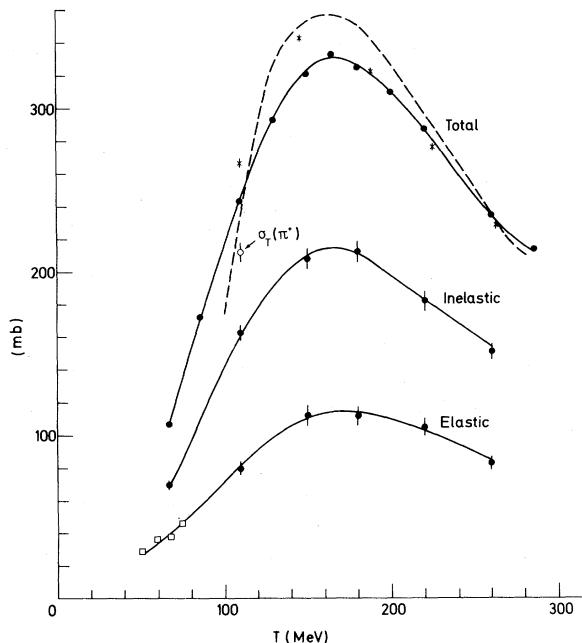


FIG. 2.  $\pi^-$ - $^4\text{He}$  total cross sections versus  $T$ , pion kinetic energy in the laboratory system. Crosses, Wilkin *et al.* (Ref. 5); squares, deduced from data of Crowe *et al.* (Ref. 6). The solid lines are a guide for the eye only. The dashed curve is a theoretical prediction by Locher, Steinmann, and Straumann (Ref. 7).

*et al.*<sup>5</sup> Measurements were made with a set of five scintillation counters with increasing diameters placed right behind the target inside the scattering chamber. The pions were tagged with a DISC counter placed just before the scattering chamber. The target was a hollow copper cylinder, 80 mm in diameter and 60 mm long, covered with thin Havar windows and filled with liquid helium. Coulomb-nuclear interference effects were corrected for by using the ratio  $\rho = \text{Re}f(0)/\text{Im}f(0)$  as deduced from our elastic scattering data. In Fig. 2 are also shown the total elastic cross sections obtained by integrating measured angular distributions and the remaining total inelastic cross sections. Points at 51, 60, 68, and 75 MeV are deduced from the data of Crowe *et al.*<sup>6</sup> Enough positive pions were available at 110 MeV for a total cross section to be computed at this energy. The curves in Fig. 2 are from a theoretical prediction by Locher, Steinmann, and Straumann.<sup>7</sup> Total cross sections agree with those of Wilkin *et al.* except for the lowest energies where the discrepancy is outside experimental errors.

Differential cross sections smoothly continue the low-energy data of Crowe *et al.*,<sup>6</sup> but they show very novel features. Firstly, the angular position of the first minimum is independent of the pion incident energy, whereas the first minimum takes place at approximately constant  $t$  in the pion- $^{12}\text{C}$  case. It probably means that in the  $^4\text{He}$  case, this minimum is connected to the zero of the spin-nonflip  $\pi$ - $N$  amplitude rather than being of a diffractive nature. Secondly, another minimum, which is wider than the first one, appears at 150 MeV and it moves towards smaller angles as the pion energy increases. Moreover, the height of the second maximum decreases by two orders of magnitude when the pion energy goes from 110 to 260 MeV, across the (3, 3) resonance, whereas it remains almost constant in the  $^{12}\text{C}$  case.<sup>1</sup>

The measured differential cross sections are fitted with the expression

$$d\sigma/d\Omega = |f_N e^{-i2\delta} + f_C|^2.$$

$f_N$ ,  $f_C$ , and  $2\delta$  are, respectively, the nuclear scattering amplitude, the Coulomb amplitude, and a standard Bethe phase.<sup>2,8</sup> Following a suggestion made by Germond and Wilkin, we chose a form of  $f_N(t)$  as

$$f_N(t) = (k/4\pi)\sigma_{\text{tot}}(i+\rho)\exp(+\frac{1}{6}R_S^2 t) \prod_j (1-t/t_j),$$

TABLE I. Fitted values for parameters of  $f_N$ .  $1-z_j = -t_j/2k^2$ ;  $n$  is the number of degrees of freedom in the fits.

$T$ (MeV)	$\rho$	$R_S$ (fm)	$\text{Re}(1-z_1)$	$\text{Im}(1-z_1)$	$\text{Re}(1-z_2)$	$\text{Im}(1-z_2)$	$n$	$\chi^2$
110	$0.560 \pm 0.047$	$1.685 \pm 0.018$	$0.704 \pm 0.009$	$0.185 \pm 0.010$	...	...	114	126
150	$0.153 \pm 0.078$	$1.238 \pm 0.131$	$0.729 \pm 0.007$	$0.137 \pm 0.010$	$2.149^{+0.876}_{-0.219}$	$-0.533 \pm 0.092$	25	29
180	$-0.023 \pm 0.031$	$1.310 \pm 0.061$	$0.708 \pm 0.008$	$-0.072 \pm 0.012$	$1.613 \pm 0.024$	$-0.372 \pm 0.055$	109	129
220	$-0.013 \pm 0.147$	$1.262 \pm 0.035$	$0.721 \pm 0.005$	$0.020 \pm 0.011$	$1.452 \pm 0.023$	$-0.202 \pm 0.031$	23	40
260	$-0.317 \pm 0.028$	$1.341 \pm 0.032$	$0.726 \pm 0.011$	$0.063 \pm 0.023$	$1.350 \pm 0.026$	$-0.119 \pm 0.051$	107	91

where the  $t_j$ 's are complex numbers. The number of factors in the product  $\prod_j$  is taken to be equal to the number of dips in the angular distributions, i.e. one at 110 MeV and below, two at 150 MeV and above. Fitted values of the parameters are given in Table I. The sign of the imaginary part is not determined by this fitting. Equally good fits can be obtained with the reverse sign.

From the values of Table I it is easy to deduce  $R$ , the slope at zero momentum transfer. The obtained values are fitted with an effective-radius-model formula,<sup>9,10</sup>  $R^2 = R_A^2 + a/k^2$  [where  $a$  equals  $\frac{3}{2}l(l+1)$  if one partial wave predominates]. One gets  $R^2 = (1.55 \pm 0.03)^2 + (4.40 \pm 0.12)/k$  which is compatible with a dominant  $p$ -wave interaction.

In Fig. 3 are shown the values of the real part of the forward-scattering amplitude  $\text{Re}f(0) = \rho(k/$

$4\pi)\sigma_{\text{tot}}$  plotted versus  $T$ . Values at 51, 60, 68, and 75 MeV were obtained by analyzing Crowe *et al.*'s data<sup>6</sup> in the way described above by using values of  $\sigma_{\text{tot}}$  extrapolated down to 51 MeV. The curves are forward-dispersion-relation calculations made by Wilkin<sup>5</sup> and by Batty, Squier, and Turner.<sup>11</sup>

We are greatly indebted to Dr. J. F. Germond and Dr. C. Wilkin for many fruitful discussions concerning the interpretation of the data. The helium target was built in the Cryogenic Department at Institut de Physique Nucléaire. We are very grateful to its chief Mr. S. Buhler, and to Mr. J. Mommejat for their devoted assistance. We thank the CERN synchrocyclotron operators. We enjoyed the help of Dr. V. Bobyr during the early part of the experiment and of Dr. E. Labie

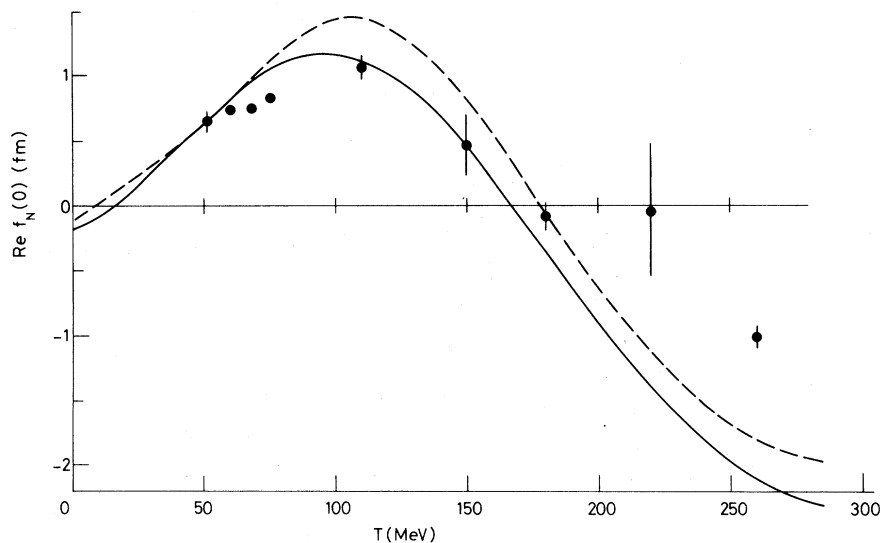


FIG. 3. Real part of the forward-scattering amplitude versus  $T$ , pion kinetic energy in the laboratory system. The curves were calculated from the forward dispersion relation by Wilkin *et al.* (Ref. 5) (dashed curve) and by Batty, Squier, and Turner (Ref. 11) (full curve).

during the last runs.

\*Now at Institut Universitaire de Technologie, Montluçon, France.

†On leave from Brookhaven National Laboratory, Upton, N. Y. 11973. Research supported by the U. S. Atomic Energy Commission.

<sup>1</sup>F. Binon, P. Duteil, J. P. Garron, J. Görres, L. Hugon, J. P. Peigneux, C. Schmit, M. Spighel, and J. P. Stroot, Nucl. Phys. **B17**, 168 (1970).

<sup>2</sup>F. Binon, V. Bobyr, P. Duteil, M. Gouanère, L. Hugon, J. P. Peigneux, J. Renuart, C. Schmit, M. Spighel, and J. P. Stroot, Nucl. Phys. **B33**, 42 (1971), and **B40**, 608(E) (1972).

<sup>3</sup>F. Binon, V. Bobyr, P. Duteil, M. Gouanère, L. Hu-

gon, M. Spighel, and J. P. Stroot, Nucl. Instrum. Methods **94**, 27 (1971).

<sup>4</sup>F. Binon *et al.*, to be published.

<sup>5</sup>C. Wilkin, C. Cox, J. Domingo, K. Gabathuler, E. Pedroni, J. Rohlin, P. Schwaller, and N. Tanner, Nucl. Phys. **B62**, 61 (1973).

<sup>6</sup>K. Crowe, A. Fainberg, J. Miller, and A. Parsons, Phys. Rev. **180**, 1349 (1969).

<sup>7</sup>M. Locher, O. Steinmann, and N. Straumann, Nucl. Phys. **B27**, 598 (1971).

<sup>8</sup>M. Locher, Nucl. Phys. **B2**, 525 (1967).

<sup>9</sup>J. Beiner and J. F. Germond, Phys. Lett. **46B**, 289 (1973).

<sup>10</sup>R. Silbar and M. Sternheim, Phys. Rev. Lett. **31**, 941 (1973).

<sup>11</sup>C. Batty, G. Squier, and G. Turner, Nucl. Phys. **B67**, 492 (1973).

## Effects of Isoscalar and Isovector Magnetic Multipole Polarizations on Single-Particle Magnetic Transitions

H. Ejiri and T. Shibata

*Department of Physics, Osaka University, Toyonaka, Osaka, Japan*

(Received 21 April 1975)

Isoscalar and isovector components of  $M2$  and  $M4$  transition matrix elements are obtained by comparing stretched single-(quasi)proton transitions with stretched single-(quasi)neutron transitions. Both the isoscalar and the isovector components are found to be smaller by factors  $g^{\text{eff}}/g \approx 0.2-0.3$  than the single-quasiparticle values. The reductions are accounted for, respectively, in terms of destructive effects of the isoscalar magnetic (spin) and the isovector magnetic (isospin-spin) core polarizations.

Recently it has been shown by Ejiri *et al.*<sup>1</sup> that isovector electric dipole ( $E1$ ) matrix elements<sup>1,2</sup> for transitions from isobaric analog states to low-lying states are uniformly smaller than single-quasiparticle values. The uniform reduction is accounted for in terms of a destructive effect of the isospin-dipole (isovector  $E1$  mode) core polarization. The Majorana-type interaction  $H_M = V_M(1 + \vec{\tau}_1 \cdot \vec{\tau}_2)(1 + \vec{\sigma}_1 \cdot \vec{\sigma}_2)f(\vec{r}_1, \vec{r}_2)$  is dominant in the exchange nuclear interaction. Consequently one may expect a spin-multipole ( $\vec{\sigma}r^\lambda \cdot \vec{Y}^\lambda$  mode) core polarization arising from the spin interaction term  $V_M \vec{\sigma}_1 \cdot \vec{\sigma}_2 f(\vec{r}_1, \vec{r}_2)$ , and an isospin-spin multipole ( $\vec{\tau} \vec{\sigma} r^\lambda \cdot \vec{Y}^\lambda$  mode) core polarization arising from the isospin-spin interaction term  $V_M \vec{\tau}_1 \cdot \vec{\tau}_2 \vec{\sigma}_1 \cdot \vec{\sigma}_2 f(\vec{r}_1, \vec{r}_2)$ , as well as the isospin-dipole ( $\vec{\tau} r^1 \cdot \vec{Y}^1$  mode) core polarization arising from the isospin interaction  $V_M \vec{\tau}_1 \cdot \vec{\tau}_2 f(\vec{r}_1, \vec{r}_2)$ . A possible reduction effect of the spin-isospin polarization has been suggested in analyses of the first forbidden  $\beta$ -decay matrix elements.<sup>3,4</sup> It is of great interest to study effects of the spin (isoscalar) and the spin-isospin (isovector) polarizations on isoscalar and isovector components of magnetic  $\gamma$  transitions between low-lying single-particle states. Quantitative investigations of  $M2$  transitions are very rare. Furthermore, separation of the isovector and the isoscalar components has been difficult since the isoscalar component itself is very small.

We studied in the present work the isoscalar and the isovector components of the  $ML$  ( $L=2, 4$ ) matrix elements by analyzing in detail both the stretched single-proton transitions and the single-neutron transitions,  $j = l + \frac{1}{2} \leftrightarrow j' = l' - \frac{1}{2}$  with  $\Delta j = L$  and  $\Delta \pi = \text{yes}$  (since the polarization with  $\Delta \pi = \text{yes}$  is essentially due to coherent  $1\hbar\omega$  particle-hole excitations, it affects uniformly transition rates between low-lying single-particle states). The stretched  $ML$  transition operator is expressed as

$$T = \frac{ke\hbar}{2mc} \left[ \left( L\mu_p - \frac{L}{L+1} \right) \frac{1-\tau_3}{2} + L\mu_n \frac{1+\tau_3}{2} \right] [\vec{\sigma} \times r^\lambda \vec{Y}^\lambda]_{L=\lambda+1}, \quad (1)$$